Journal of Geoscience and Environment Protection, 2023, 11, 37-51
https://www.scirp.org/journal/gep
ISSN Online: 2327-4344
ISSN Print: 2327-4336

Radiometric and Geophysical Investigations on Exposure Levels and Excess Cancer Risk in Kargi-Kenya

Willis O. Aguko, Robert Kinyua, John G. Githiri

Physics Department, School of Physical Sciences, College of Pure & Applied Sciences, Jomo Kenyatta University of Agriculture and Technology, Nairobi, Kenya
Email: agukow8@gmail.com, agukow@kebs.org, kinyua@fsc.jkuat.ac.ke, githiri@fsc.jkuat.ac.ke

How to cite this paper: Aguko, W. O., Kinyua, R., & Githiri, J. G. (2023). Radiometric and Geophysical Investigations on Exposure Levels and Excess Cancer Risk in Kargi-Kenya. *Journal of Geoscience and Environment Protection, 11,* 37-51.
https://doi.org/10.4236/gep.2023.114004

Received: February 19, 2023
Accepted: April 23, 2023
Published: April 26, 2023

Copyright © 2023 by author(s) and Scientific Research Publishing Inc.
This work is licensed under the Creative Commons Attribution International License (CC BY 4.0).
http://creativecommons.org/licenses/by/4.0/
Open Access

Abstract

Radiation is considered one of the possible causes of cancer disease with natural background sources including cosmic, terrestrial and internal radiation. A number of cancer disease cases have been reported in Kargi with their causes not properly documented. The present work characterized the radioactivity in soil and water, to find out possible causes of radiation in KARGI-KENYA by studying magnetic intensities, anomalous zones with depth to magnetic sources and delineating subsurface structures. A total of 117 soil and 14 water samples were collected from the entire area and analysed for radionuclides due to ^{40}K, ^{232}Th and ^{226}Ra. Measurement methods of proton magnetometer and gamma spectrometry employing a high purity germanium (HPGe) detector were employed basically to evaluate the magnetic survey and radiological hazard of radioactivities respectively. A total of 51 magnetic field measurements were taken on the eastern part of Kargi, a place suspected to have more concentration of radionuclides. The results showed that there could have been a fractionation during weathering period or metasomatic activity of the radioelements involvement. This study also reveals that the mining activities in the nearby study area could have affected the geologic formation causing more fracturing in rocks and pronounced subsurface structures as a result of mining that could have served as passage for leachates from pollutants as well as the level of radiation in the study area.

Keywords

Kargi, Magnetic Survey, Anomalous zones, Geologic, Germanium Detector

1. Introduction

Radiation is considered one of the possible causes of cancer disease. Radiation

dose, however small it can be, is still harmful to health. Kargi has reported a number of cancer disease cases and abrupt animal deaths interfering with the healthy status of this area. Soil radionuclide activity concentration is considered major determinant of natural background radiation. Disintegration of rocks via natural and man-made processes helps radionuclides to be carried to soil by rain or water flows (Okpoli & Akingboye, 2016). Concentrations of natural radioactivity mainly depend on geographical and geological conditions appearing at different levels in soils of different geological regions. For out-door occupation evaluating terrestrial gamma dose-rate, approximation of the natural radioactivity extent is very important for geological samples, usually ascertained from the ^{40}K, ^{232}Th and ^{226}Ra contents (UNSCEAR, 2000). The search for causes of cancer is therefore paramount in order to help the health community control on the disease and better health practices adviced as far as this disease is concerned.

Human beings and animals are unprotected by food chain pollution happening as a result of radionuclides deposits on plant leaves, roots uptake from polluted soil, water and/or sediment (Arogunjo et al., 2004) and also from direct consumption of polluted waters (Avwiri & Agbalagba, 2007).

Researcher Otton (1994) gives an explanation that between lower and moderate radiation doses, exposure to radiation both in human and animal may give rise to long term cancer disease occurrence and that the rate of genetic abnormal formations may rise by exposing to radiation. It is of importance therefore to discover the existing quantity of radioactivity in soil and drinking water for every area of residence in order to protect against its harmful effects (WHO, 2008).

To comprehend the area's subsurface geology for detailed mapping, magnetic method (ground based) is used. This technique has extensively been employed in basement mapping (Folami, 1992). The technique needs measurement of the magnetic components amplitude at distinct points along traverses regularly distributed throughout the interest area of survey. Three components are measured in ground magnetic study, and include horizontal, vertical together with total components. The vertical components are mostly applied in the past studies to delineate fractures, faults, depth to magnetic basement together with other structures (Nettleton, 1976).

The aim of this work is to find out possible causes of radiation in this area by studying magnetic intensities, delineating subsurface structures, anomalous zones with depth to magnetic sources and to gauge radiological health hazard together with environmental radioactivity.

2. Study Area

Figure 1 shows the studied area. Kargi, approximately 70 km west of Marsabit town is in Marsabit county, Laisamis constituency and Loiyangalani sub-county. Kargi borders chalbi, Gabra and Samburu. The area under study, located between 2˚28'37"N and 2˚31'15"N & 37˚32'34"E and 37˚36'07"E is approximately 31 km^2.

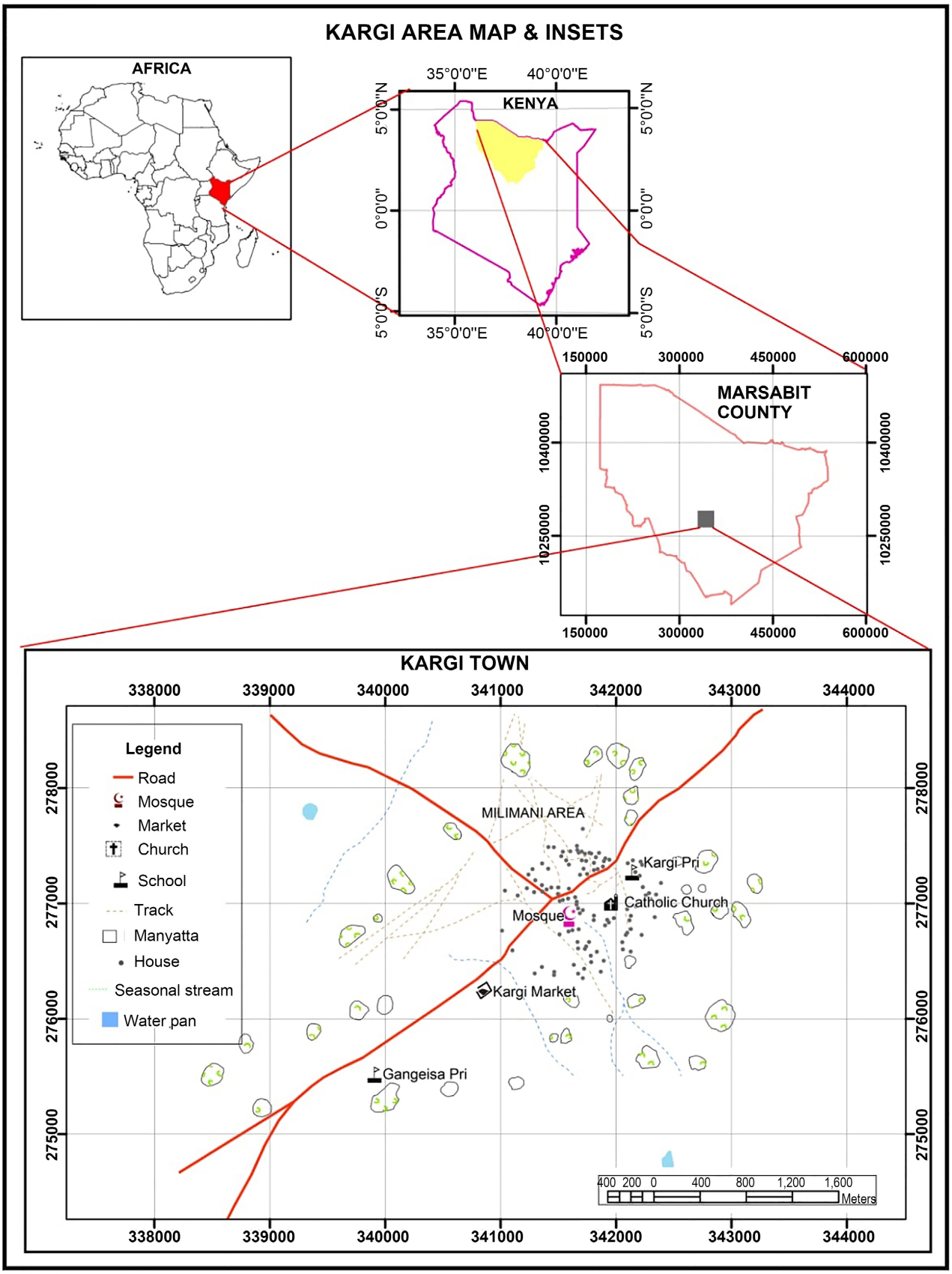

Figure 1. Study area (Aguko et al., 2020).

3. Geology of Kargi

Geology of study area is contained in sheet 20, a remote 12,200 km^2 tract of the northern Kenya which was geologically mapped and geochemically surveyed at a reconnaissance scale in late 1984 by use of helicopter support. The sheet is bounded by both latitudes and longitudes 1˚N and 3˚N and 37˚E and 38˚E respectively (Report 108 (Reconnaissance), 1987) as seen from **Figure 2**.

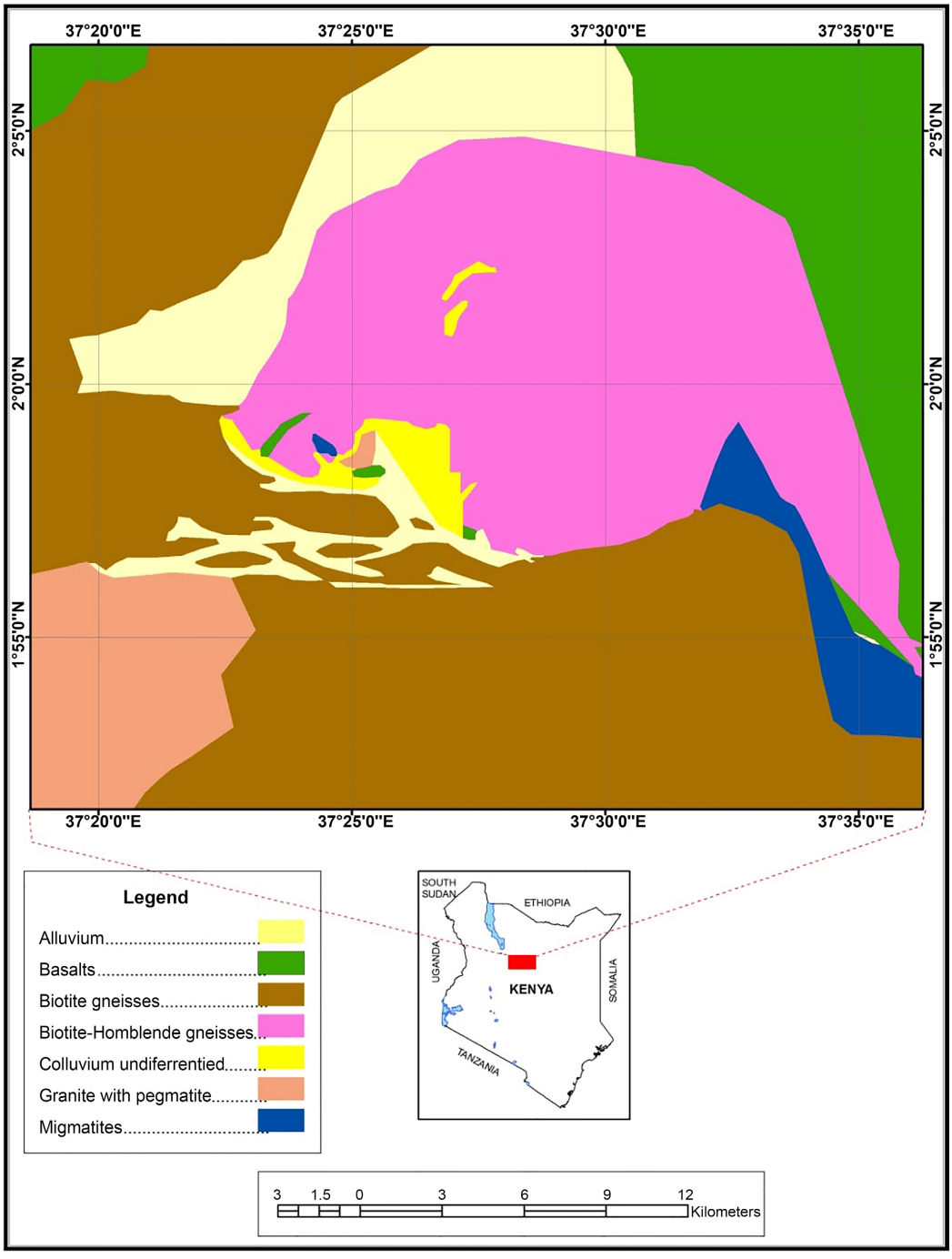

Figure 2. Four major volcanic shields and their position relative to the rift faulting. Trends of pyroclasticcentres within shields shown by continuous straight lines.

From the report, Kargi is covered by Basalt capped mesas rocks which never rise more than 50 m above the adjacent plain and consists of a thin (less than 20 m) basalt cap invariably overlying sedimentary rock. A monotonous soil, rich in sand mantles the flat floor of the desert. However, there are subdued sand mounds suggesting that the area may formerly have been part of an extensive dune field. Near Kargi, re-activation of sand is giving rise to new dunes. These are relatively small longitudinal dunes parallel to the prevailing WNW directed winds (Report 108 (Rconnaisance), 1987).

Algas Basalt, near Kargi on the western margin of the Marsabit lava dates to 2.5 ± 0.3 Ma. Basalt rocks contain plagioclase feldspar which is rich in radioactive minerals. Plagioclase feldspar is a member of feldspar group originating from igneous rocks (Report 108 (Rconnaisance), 1987). Feldspar is from granite rocks, which are considered rich in minerals. Two main groups of feldspar are Potassium feldspar ("K-spar") and plagioclase ("plag"). Potassium (Potassic feldspar), Uranium (Uraninite, Urathorite, etc) and Thorium (Monazite, Zircon, etc) bearing minerals are traced to this rock type.

4. Sampling, Materials and Measurements

117 and 14 soil and water samples respectively were collected from Kargi, with 51 magnetic measurements done on the eastern side of study area, a place suspected to have more radionuclides (IAEA TECDOC 486, 2019). EPA (1995), describes factors determining the distances between sampling points in the grid as the area to be sampled together with the number of samples. For soil sampling, systematic grid sampling, considered unbiased sampling method was employed. By dividing the area in to regular squares each of about 500.0 m × 500.0 m, the area was marked to aid get a better sampling representation. Soil samples were collected from the nodes (**Figure 2**). To avoid soil samples contamination from surface with leaves and other contaminants, samples were collected approximately 10 centimetres from the soil surface (Monika et al., 2010).

Kargi water sources are categorized as boreholes (shallow wells), Tap/Water kiosks and dams/wells. Water samples were drawn from these sources in standard polyethylene (0.5 litre) Marinelli containers, packaged and well-marked before laboratory transportation. These containers were washed clean before rinsing with diluted hydrochloric acid and distilled water respectively before filling with collected water samples. Concentrated Nitric acid (HNO_3), 0.25 ml was added to the collected water samples to help preventing any loss of radium isotopes around the walls of the container and to avoid growth of micro-organisms (Hany & Abdallah, 2014). The containers were bream-filled and tightly closed not to allow any air inside.

All the collected water samples were clearly marked, laboratory transported for further preparation and analysis. **Figure 3** and **Figure 4** give soil samples and magnetic reading plans while **Table 1** shows sources of water samples collection, activity concentrations and Radium equivalent values and their locations in the map. Again, **Figure 4** shows magnetic anomaly for the area.

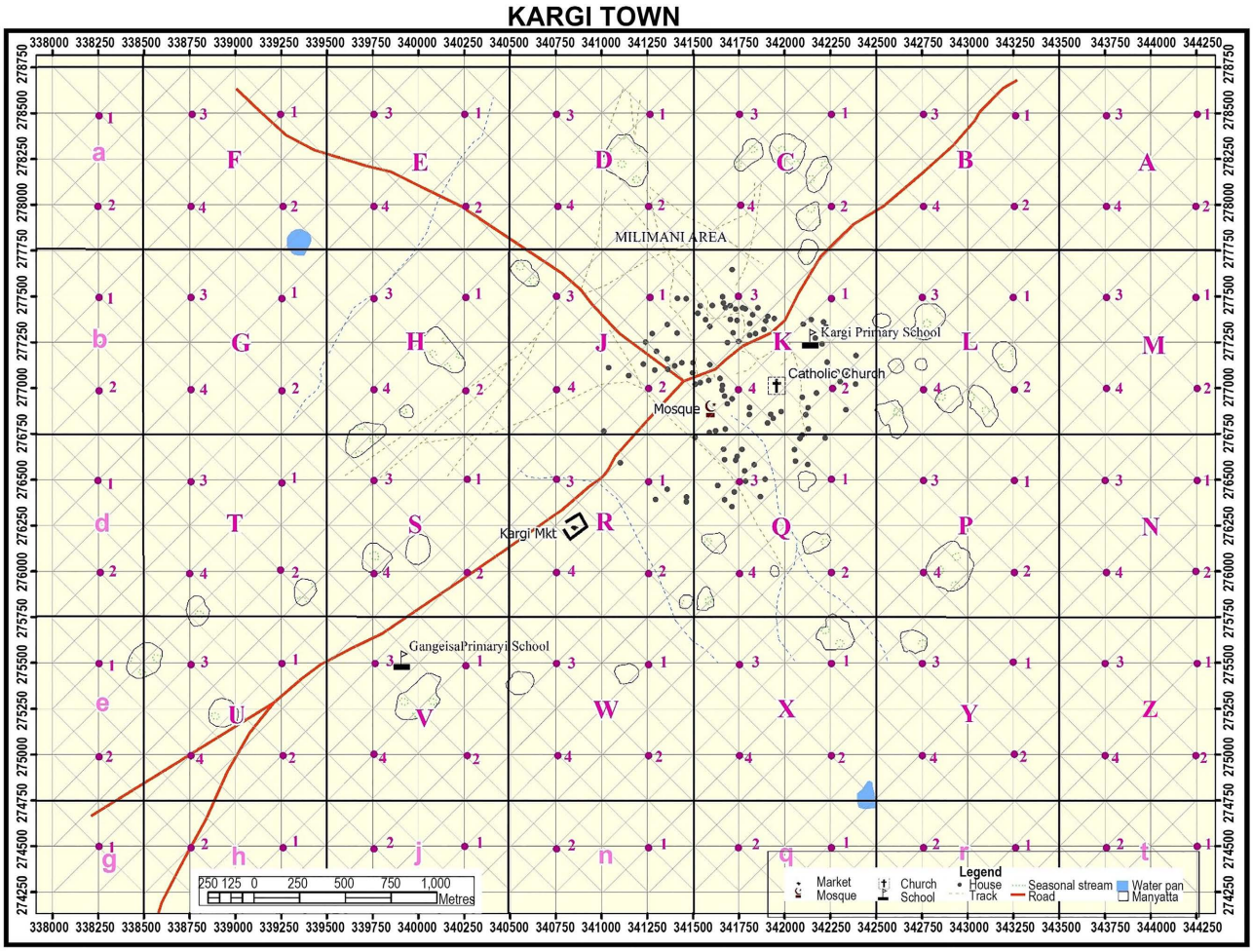

Figure 3. Soil sample collection plan for Kargi (Aguko et al., 2020).

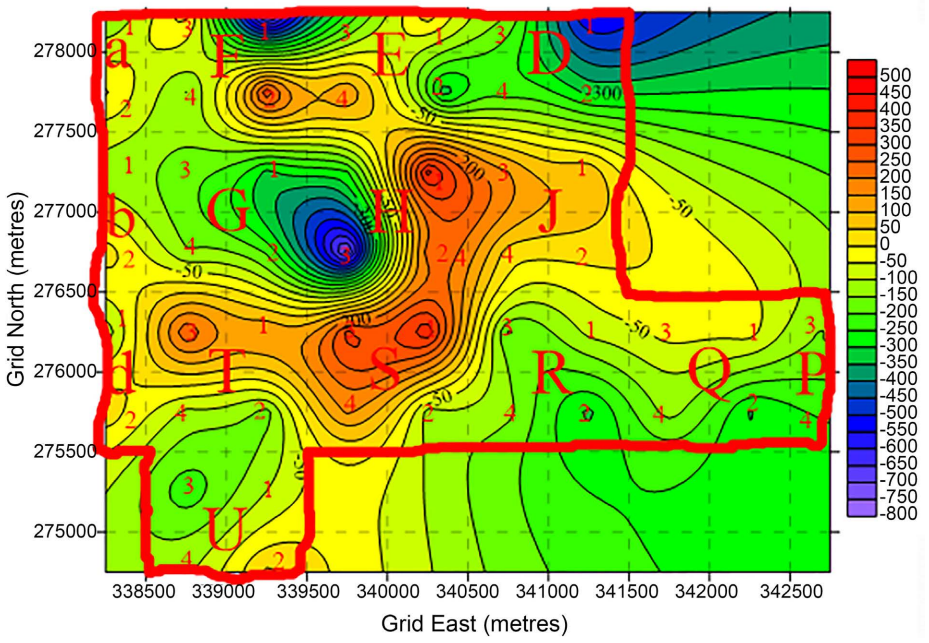

Figure 4. Plotted Magnetic anomaly map for Kargi.

Table 1. Water sample code, location, average activity concentration ($Bq \cdot l^{-1}$) and Radium equivalent ($Bq \cdot l^{-1}$).

Sample code	LOCATION		Average activity Concentration, $Bq \cdot l^{-1}$			Ra_{eq}, $Bq \cdot kg^{-1}$
	(Longitude) Easting, E	(Latitude) Northing, N	^{226}Ra	^{232}Th	^{40}K	
W_1	37.591971	2.517675	3.63 ± 2.79	0.12 ± 2.12	71.33 ± 10.81	9.29
W_2	37.596068	2.503742	4.55 ± 1.81	2.64 ± 2.14	54.63 ± 8.67	12.53
W_3	37.583479	2.495335	7.84 ± 5.05	1.71 ± 6.03	36.01 ± 28.50	13.06
W_4	37.58304	2.485123	2.08 ± 2.19	0.98 ± 3.16	68.92 ± 9.92	8.79
W_5	37.549452	2.486624	3.39 ± 4.39	7.99 ± 4.61	57.72 ± 24.74	19.26
W_6	37.553105	2.492507	6.04 ± 2.18	3.94 ± 3.76	77.16 ± 14.58	17.62
W_7	37.568392	2.509391	5.66 ± 2.40	−2.00 ± 2.37	45.68 ± 19.38	6.32
W_8	37.56921	2.501813	6.41 ± 2.85	1.90 ± 3.07	64.45 ± 14.13	14.09
W_9	37.569227	2.501994	7.66 ± 2.97	4.37 ± 3.95	60.49 ± 19.75	18.57
W_{10}	37.570479	2.492526	0.59 ± 2.01	3.12 ± 3.16	42.33 ± 14.70	8.30
W_{11}	37.570588	2.499644	3.59 ± 2.21	0.19 ± 2.81	72.53 ± 11.57	9.45
W_{12}	37.570606	2.499707	0.27 ± 2.63	0.54 ± 3.85	−2.36 ± 13.22	0.84
W_{13}	37.576149	2.503919	−1.82 ± 3.42	6.09 ± 4.74	81.22 ± 22.00	13.14
W_{14}	37.575952	2.503693	−0.25 ± 2.70	−0.85 ± 2.55	7.61 ± 12.69	-0.88
	Average		**3.55 ± 3.04**	**2.20 ± 2.74**	**52.68 ± 25.07**	**10.74 ± 6.03**

5. Results and Discussion

For radiometric results, Table 1 and Table 2 for water and soil respectively give mean activity concentrations and radium equivalent values for Kargi. For water samples analysed, ^{40}K, ^{238}U, ^{232}Th and Ra_{eq} values ranged from −2.36 ± 13.22 to 81.22 ± 22.00, −1.82 ± 3.42 to 7.84 ± 5.05, −2.00 ± 2.37 to 7.99 ± 4.61 and −0.88 to 19.26 $Bq \cdot l^{-1}$ respectively with arithmetic mean and standard deviation of 52.68 ± 25.07, 3.55 ± 3.04, 2.20 ± 2.74 and 10.74 ± 6.03 $Bq \cdot kg^{-1}$ respectively. Soil samples analysis yielded for ^{40}K, ^{238}U, ^{232}Th and Ra_{eq} values from 231.27 ± 86.67 to 450.12 ± 52.19, 4.04 ± 1.05 to 11.96 ± 2.81, 2.74 ± 2.59 to 12.34 ± 3.14 and 33.24 ± 3.40 to 58.57 ± 18.03 $Bq \cdot kg^{-1}$ respectively with arithmetic mean and standard deviation of 354.81 ± 67.06, 7.23 ± 1.67, 8.03 ± 1.91 and 46.04 ± 6.28 $Bq \cdot kg^{-1}$ respectively. Globally, recommended values for soil activities are respectively 37.0 $Bq \cdot kg^{-1}$, 33.0 $Bq \cdot kg^{-1}$, 400.0 $Bq \cdot kg^{-1}$ (UNSCEAR, 2008) and 370 $Bq \cdot kg^{-1}$, while for water are respectively 10.0 $Bq \cdot l^{-1}$, 1.0 $Bq \cdot l^{-1}$, 10.0 $Bq \cdot l^{-1}$ (UNSCEAR, 2000; WHO 2008 Standards) and 370 $Bq \cdot kg^{-1}$ as per Organization for Economic Cooperation and Development, OECD.

Figure 5 and Figure 6 give a summary of activity concentrations for water and soil respectively.

All calculated mean activities for ^{232}Th, ^{226}Ra, ^{40}K and Ra_{eq} from the soil were found less than the global values recommended. Mean calculated absorbed dose rates for all collected soil samples was 23.87 ± 3.48 nGy/h against the global

Table 2. Soil sample collection plan, average activity concentration ($Bq \cdot l^{-1}$) and Radium equivalent ($Bq \cdot l^{-1}$).

Sample area code	Number of water samples collected	Sampling area, km^{20}	Activity, Bq/kg			Radium equivalent activity, (Ra_{eq}) in $Bq \cdot kg^{-1}$
			^{232}Th	^{238}U	^{40}K	
A	4	1.00	4.32 ± 2.04	5.80 ± 1.92	276.14 ± 46.70	33.24 ± 3.40
B	4	1.00	5.63 ± 1.86	6.78 ± 2.25	405.39 ± 84.53	46.04 ± 5.52
C	4	1.00	7.03 ± 2.29	6.08 ± 1.23	324.42 ± 70.37	41.11 ± 4.75
D	4	1.00	8.42 ± 2.23	6.83 ± 1.59	287.93 ± 76.28	41.04 ± 8.04
E	4	1.00	10.07 ± 4.31	6.75 ± 3.02	281.74 ± 119.85	42.84 ± 14.55
F	4	1.00	9.35 ± 5.51	8.86 ± 1.60	361.70 ± 117.59	50.08 ± 18.37
G	4	1.00	8.96 ± 3.21	7.77 ± 1.44	455.26 ± 101.45	55.64 ± 7.39
H	4	1.00	6.97 ± 3.65	7.89 ± 1.30	259.89 ± 54.69	37.86 ± 6.61
J	4	1.00	8.43 ± 0.33	6.30 ± 1.82	242.56 ± 89.52	37.03 ± 7.61
K	4	1.00	6.84 ± 1.12	9.75 ± 5.62	287.13 ± 98.99	41.64 ± 13.41
L	4	1.00	6.62 ± 2.61	5.93 ± 0.70	436.01 ± 40.84	48.96 ± 6.08
M	4	1.00	6.37 ± 0.68	5.71 ± 1.16	330.39 ± 21.92	40.25 ± 1.65
N	4	1.00	9.70 ± 5.47	6.13 ± 0.68	308.68 ± 116.39	43.76 ± 16.76
P	4	1.00	2.74 ± 2.59	6.07 ± 2.40	349.51 ± 70.58	36.91 ± 2.73
Q	4	1.00	9.70 ± 3.70	8.51 ± 2.73	405.47 ± 155.79	53.60 ± 17.31
R	4	1.00	7.49 ± 2.78	8.72 ± 2.26	398.65 ± 33.46	50.13 ± 6.43
S	4	1.00	6.71 ± 1.63	7.93 ± 0.24	330.12 ± 49.75	42.94 ± 3.89
T	4	1.00	10.66 ± 5.89	10.53 ± 3.51	425.98 ± 131.73	58.57 ± 18.03
U	4	1.00	8.33 ± 3.20	7.73 ± 1.75	380.98 ± 168.08	48.97 ± 16.99
V	4	1.00	8.96 ± 12.51	6.36 ± 3.62	440.90 ± 151.62	53.12 ± 32.96
W	4	1.00	6.54 ± 4.26	6.85 ± 1.33	450.12 ± 52.19	50.86 ± 9.57
X	4	1.00	9.34 ± 5.98	9.05 ± 4.68	380.08 ± 264.93	51.67 ± 29.07
Y	4	1.00	9.31 ± 5.13	11.96 ± 2.81	231.27 ± 86.67	43.07 ± 11.16
Z	4	1.00	12.34 ± 3.14	8.53 ± 2.09	311.59 ± 33.34	50.17 ± 5.64
a	2	0.50	7.70 ± 0.86	5.61 ± 1.61	438.06 ± 143.71	50.34 ± 10.68
b	2	0.50	9.75 ± 5.96	5.54 ± 0.32	472.49 ± 57.64	55.85 ± 3.77
d	2	0.50	8.73 ± 4.47	4.04 ± 1.05	369.76 ± 115.25	45.00 ± 1.44
e	2	0.50	6.98 ± 0.07	6.78 ± 1.77	404.28 ± 82.71	47.89 ± 8.24
g	1	0.25	9.89 ± 0.00	5.75 ± 0.00	407.13 ± 0.00	51.24 ± 0.00
h	2	0.50	8.65 ± 0.64	8.58 ± 2.57	387.28 ± 42.80	50.76 ± 6.78
j	2	0.50	9.83 ± 0.14	6.12 ± 2.27	372.98 ± 32.05	48.89 ± 0.40
n	2	0.50	6.87 ± 0.69	7.61 ± 0.08	333.28 ± 32.51	43.09 ± 1.59
q	2	0.50	5.18 ± 0.71	6.46 ± 2.55	286.89 ± 11.60	35.95 ± 4.46
r	2	0.50	8.54 ± 1.34	4.94 ± 1.21	324.75 ± 10.59	42.15 ± 1.53
t	2	0.50	8.27 ± 2.07	8.78 ± 1.49	259.57 ± 128.33	40.58 ± 11.35
Total	117	**Average**	8.03 ± 1.91	7.23 ± 1.67	354.81 ± 67.06	46.04 ± 6.28

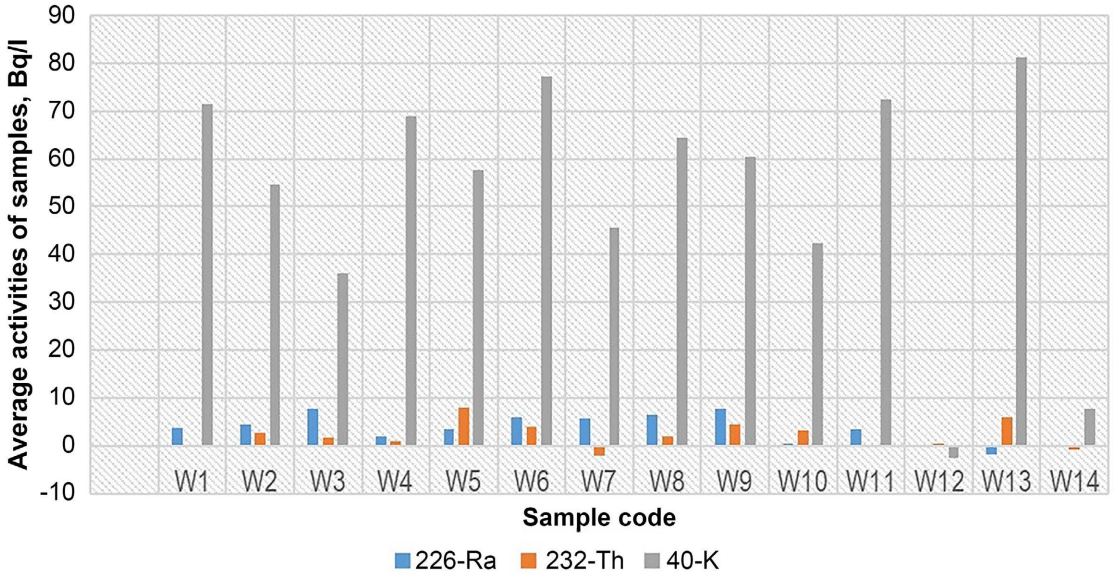

Figure 5. Activity values of samples due to ^{226}Ra, ^{232}Th and ^{40}K in investigated area, water samples.

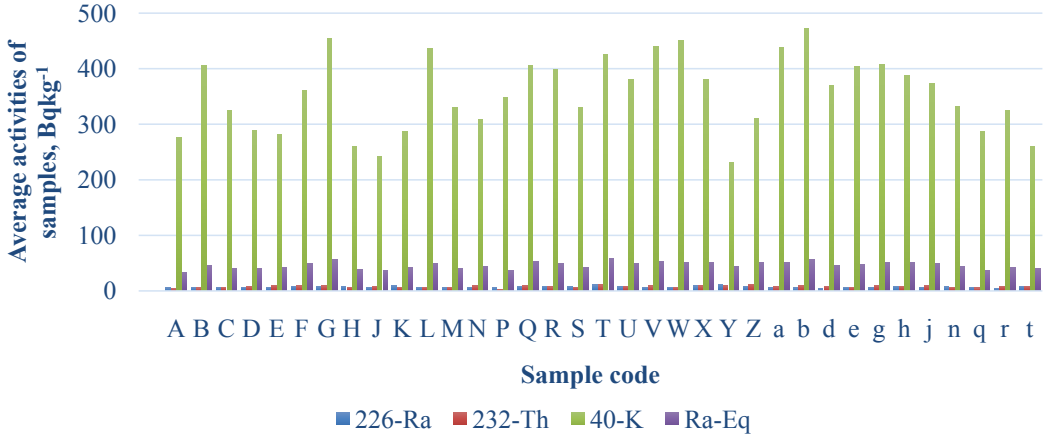

Figure 6. Activity values of samples due to ^{226}Ra, ^{232}Th, ^{40}K together with Ra_{eq} in Kargi, Soil.

median value (UNSCEAR, 2000) of 54 nGy/h. These values ranged between 16.06 ± 1.09 and 29.35 ± 1.32 nGy/h. For water results, the mean activities for the area studied was 5 times higher, low, 2 times higher and low against the worldwide accepted limit for ^{40}K, ^{226}Ra, ^{232}Th and Ra_{eq} respectively.

The AEDE (De) values as calculated from soil samples, were found lower than the world acceptable value of 1 $mSv{\cdot}y^{-1}$ (ICRP, 2000) with an average and standard deviation of 0.14 ± 0.03 $mSv{\cdot}y^{-1}$, ranging from 0.11 ± 0.01 to 0.18 ± 0.06 mSv/y. Excess lifetime cancer risk, an added risk that a person might have on contracting cancer disease if susceptible for extended period to cancer disease causing materials. By using 70 years as average life duration taking a risk factor of 0.05 per Sv (ICRP, 2007; Taskin et al., 2009) and a median annual effective dose rate of 0.14 mSv/y, then excess cancer risk is computed as 0.05%. This value is less than global value of 0.145% (Taskin et al., 2009; UNSCEAR, 2000).

Tzortzis & Tsertos (2004) and Al-Hamarneh & Awadalla (2009) pointed that a low or high value of Th/U ratios as measured in some studied locations may be an indication of a depletion in uranium or thorium enrichment due to alteration of natural processes in that particular area. They approximated the theoretical normal continental crust values of Th/U elemental ratios to be 3.0. From the study, Th/U calculated results varied from 1.19 ± 0.85 to 6.35 ± 1.72 with mean and standard deviation of 3.57 ± 1.13. Other calculated correlation ratios of K/U together with K/Th varied from 0.84 ± 0.46 to 3.89 ± 2.13 together with 0.34 ± 0.09 to 1.94 ± 2.42 with average and standard deviations of 2.15 ± 0.67 and 0.68 ± 0.30 respectively. Correlations existing between activities ^{232}Th and ^{238}U, ^{40}K and ^{238}U and ^{40}K and ^{232}Th displayed a weak relationship existing on ^{232}Th against ^{238}U, ^{40}K against ^{232}Th together with ^{40}K against ^{238}U with correlation coefficients of 0.405, 0.319 and 0.134 respective.

6. Magnetic Maps

The obtained magnetic data along traverses at the eastern side of Kargi was used in producing Total magnetic intensity (TMI) map to help deduce the magnetic intensity range of the rocks with geologic structures and areas that are susceptible. An amplitude range between −791.4 nT and 419.9 nT for the Total magnetic intensity map was seen. These values are not uncommon in a basement complex (Telford et al., 1990). Due to the mineral content in the surface and sub-surface rocks and its structural mapping, the total magnetic intensity ranges from one location to another. **Figure 7** shows the Total magnetic intensity (TMI) maps for studied area. Areas denoted by A, B and C are areas considered to have high amplitude of magnetic intensity; suggesting the presence of the basement rocks occurring at shallow depth below the surface. Areas with the low negative amplitude in magnetic intensity marked D is an area indicating the zones of weaknesses that suggest the presence of geologic structures like fractures, faults and lineaments.

The ranging magnetic intensity suggests ranging magnetic materials associated with the rock types in the area. According to Gunn et al., 1997a, the amplitude of a magnetic anomaly is directly proportional to magnetization and depends on magnetic susceptibility of the rocks.

The Tilt Derivative (TDR) together with its Horizontal component (HD_TDR) maps for area under study were derived from the tilt derivative filter applied to the TMI grids to establish fault & folds, the contacts & edges or boundaries of magnetic sources as in **Figure 8** and **Figure 9**, and to intensify both weak and strong magnetic anomalies of the area placing an anomaly directly over its source. Tilt angle derivative (TDR) of TMI establishes the edges of formations and especially at shallow depths by using a theory that zero-contours are the edges of the formation (Salem et al., 2007). It is observed that the zero contours estimate the location of abrupt changes in magnetic susceptibility values. The zero contour lines are represented by yellow colour, areas which show the lineaments are those

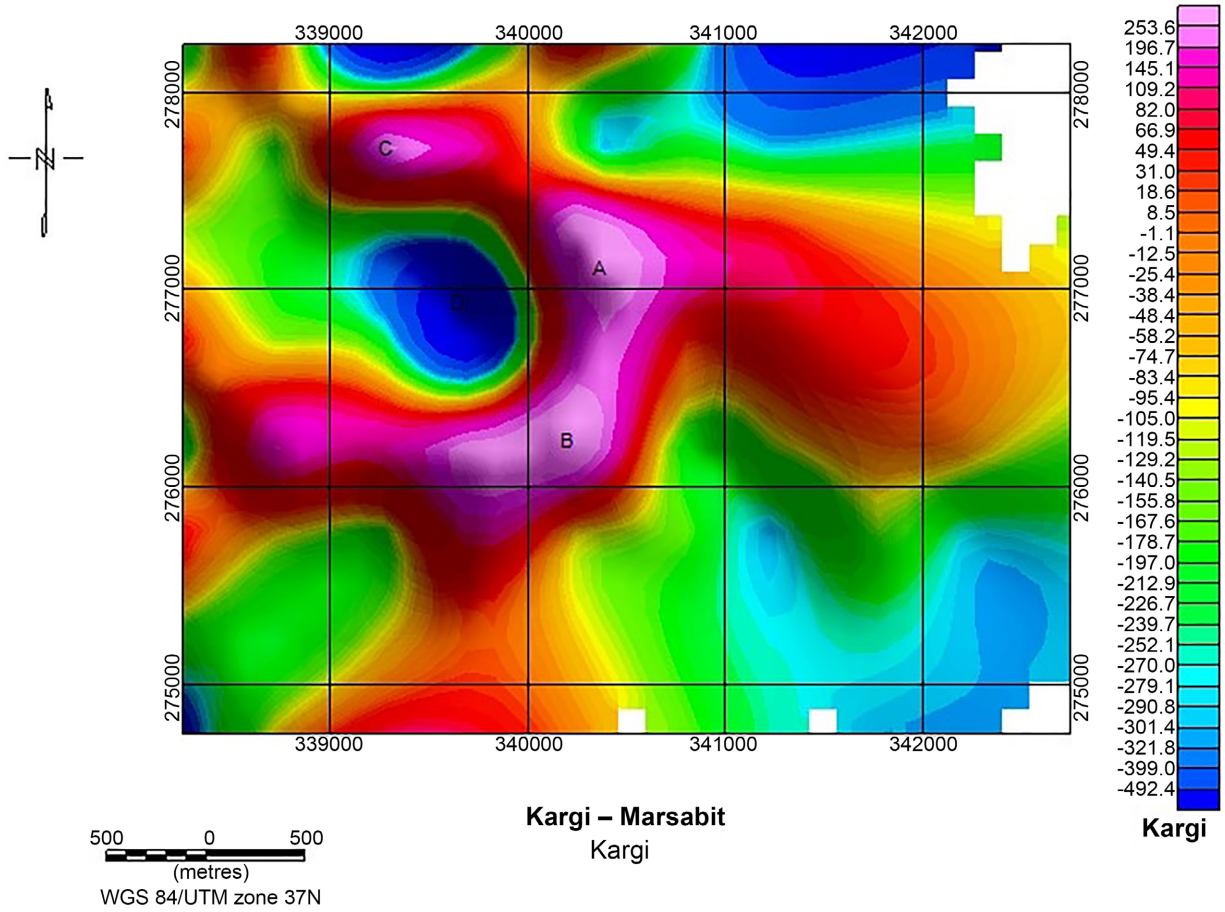

Figure 7. Total magnetic intensity (TMI) map of Kargi area.

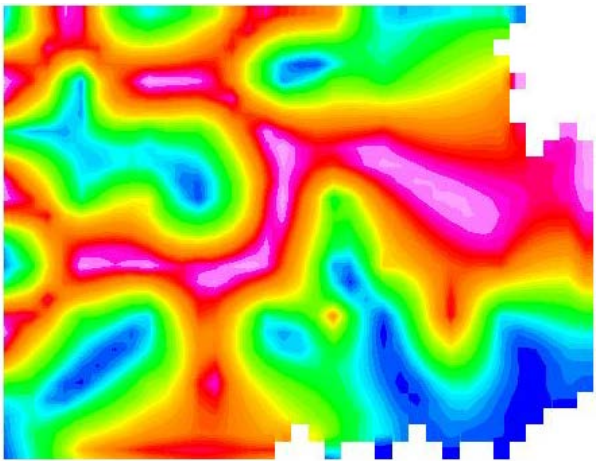

Figure 8. Tilt angle derivative (TDR) derived from TMI of the Study Area.

with blue colour, while those with red are the un-deformed or un-weathered basement. Figure 8 shows the resolution of the tilt angle derivative (TDR) in the vertical direction while Figure 9 shows the resolution of the tilt angle derivative (TDR) in the horizontal direction of the study area. Comparing Figure 8 and Figure 9, the TDR image shows different lineaments and contacts in the area.

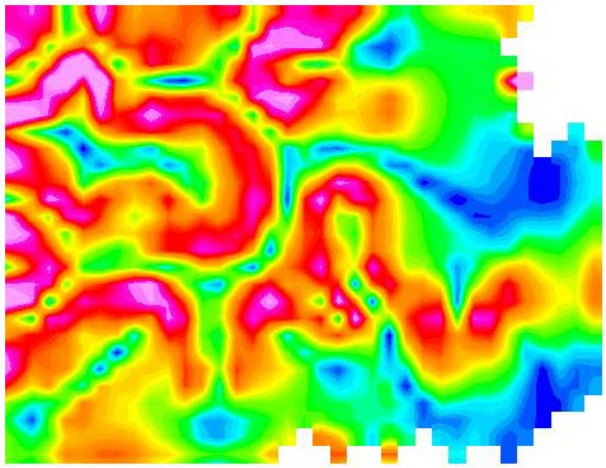

Figure 9. Tilt angle derivative (HD_TDR) in the horizontal direction derived from TMI of the Study Area.

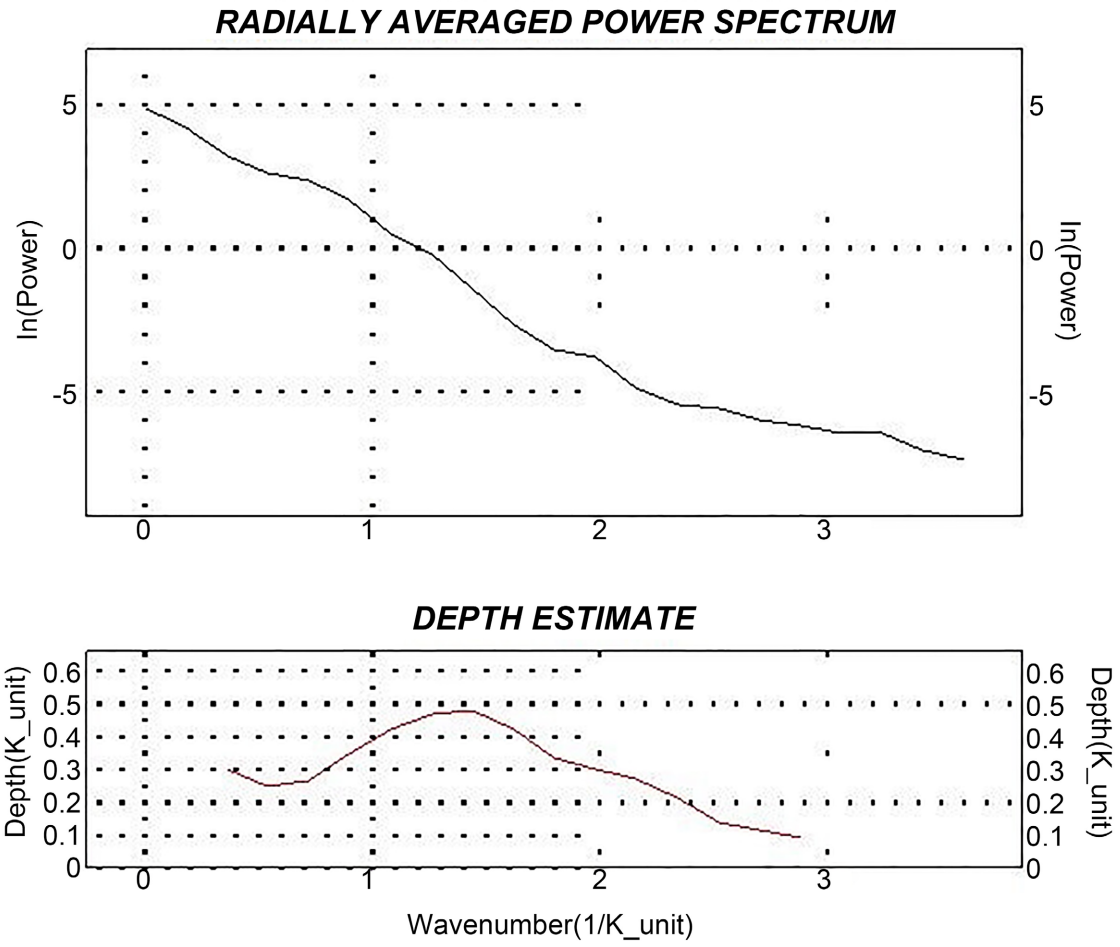

Figure 10. Radially Averaged Power Spectrum (RAPS) and Depth Estimate.

Figure 10 shows the Radial Average Power Spectrum (RAPS) of the study area with the total depth estimate to the top of geologic sources that produced the observed anomalies in the magnetic map and were ascertained using spectral

analysis. For the study area, the depths to the magnetic sources range from 100 m to 480 m. The depths of the anomalous bodies in in the area showed that the anomalous bodies are very close to the surface because the depth estimations from the power spectrum is indicating near surface of the bodies.

7. Recommendation

We recommend that further studies in Kargi area especially on the radiation source be done and especially where magnetic readings were not taken. This will help understand from which sources the available radiation come from.

8. Conclusion

The study has shown the importance and worthiness of radiometric and magnetics methods in effective mapping out of lithologies, characterizing magnetic intensities and radionuclides, delineating subsurface structures¸ anomalous zo magnetic sources. The varying magnetic intensity suggests varying magnetic materials associated with the rock types in the area. The radiometric profiles established evidences from the geologic formations about the radiation levels of the area under investigation. Geologic events like intensive weathering of the feldspar-bearing-minerals in parent rocks into clay particles have been eroded from their source and low enrichment of the parent rocks in potassic feldspar in relation to other feldspar minerals must have caused the radioactivity level K, U and Th in area.

The elevated radiation level of ^{40}K in some parts of the western side of Kargi with some ^{238}U and ^{232}Th, suggests that the geologic formation of the area is richer in potassium-bearing minerals, Uranium-bearing-minerals and Thorium bearing-minerals respectively. Weathering rate of the parent rocks, terrestrial gamma radiation enrichment in parent rocks, and low fracturing density system of the parent rocks that would have accumulated materials that are non-radioactive could all have accounted for the radioactivity level of the area. Because Th/U calculated value was greater than the recommended, it can be concluded from the study that there could have been a fractionation during weathering period or metasomatic activity of the radioelements involvement. This study also reveals that the mining activities in the nearby study area could have affected the geologic formation causing more fracturing in rocks and pronounced subsurface structures as a result of mining that could have served as passage for leachates from pollutants as well as the level of radiation in the study area.

Nevertheless, the results from analyzed soil and water samples from the study area when compared with international standard show that the area is safe to humans for agricultural practices, drinking, mining and domestic purposes.

Conflicts of Interest

The authors declare no conflicts of interest regarding the publication of this paper.

References

Aguko, W., Kinyua, R., & Githiri, J. (2020). Natural Radioactivity and Excess Lifetime Cancer Risk Associated with Soil in Kargi Area, Marsabit-Kenya. *Journal of Geoscience and Environment Protection, 8,* 127-143. https://doi.org/10.4236/gep.2020.812008

Al-Hamarne, I. F., & Awadallah, M. I. (2009). Soil Radioactivity Levels and Radiation Hazard Assessment in the Highlands of Northern Jordan. *Radiation Measurements, 44,* 102-110. https://doi.org/10.1016/j.radmeas.2008.11.005

Arogunjo, A. M., Farai, I. P., & Fuwape, I. A. (2004). Impact of Oil and Gas Industry on the Natural Radioactivity Distribution in the Delta Region of Nigeria. *Nigeria Journal of Physics, 16,* 136.

Avwiri, G. O., & Agbalagba, E. O. (2007). Survey of Gross Alpha and Gross Beta Radionuclide Activity in Okpare-Creek, Delta State, Nigeria. *Asian Journal of Applied Science, 7,* 3542-3542. https://doi.org/10.3923/jas.2007.3542.3546

EPA (1995). *Representative Sampling Guidance, Vol. 1: Soil*. EPA/540/R-95/141, EPA, Washington DC.

Folami, S. L. (1992). Interpretation of Aero Magnetic Anomalies in Iwaraja Area, Southwestern Nigeria. *Journal of Mining and Geology, 28,* 391-396.

Gunn, P., Maidment, D., & Milligan, P. (1997a). Interpreting Aeromagnetic Data in Areas of Limited Outcrop. *AGSO Journal of Australian Geology & Geophysics, 17,* 175-185.

Hany, E., & Abdallah, I. A. E. (2014). Natural Radioactivity in Water Samples from Assiut City, Egypt. *International Journal of Pure and Applied Sciences and Technology, 22,* 44-52.

IAEA TECDOC 486 (2019). *Guidelines on Soil and Vegetation Sampling for Radiological Monitoring*. International Atomic Energy Agency.

ICRP (2000). *Protection of the Public in Situations of Prolonged Radiation Exposure* (ICRP Publication 82, Ann. ICRP, Vol. 29, pp. 1-2). Pergamon.

ICRP (2007). *The 2007 Recommendations of the International Commission on Radiological Protection*.

Ministry of Environment and Natural Resources, Mines and Geological Department, Republic of Kenya (1987). *Report 108 (Rconnaisance)*.

Monika, S., Leszek, P., & Marcin, Z. (2010). Natural Radioactivity of Soil and Sediment Samples Collected from Postindustrial Area, Poland. *Polish Journal of Environmental Studies, 19,* 1095-1099.

Nettleton, L. L. (1976). *Gravity and Magnetics in Oil Prospecting* (pp. 394-413). McGraw-Hill.

Okpoli, C. C., & Akingboye, A. S. (2016). Magnetic, Radiometric and Geochemical Survey of Quarry Sites in Ondo State, Southwestern, Nigeria. *International Basic and Applied Research Journal, 2,* 16-30.

Otton, J. K. (1994). *National Radioactivity in Environment*. http://energy.usgs.gov/factsheets/radioactivity

Salem, A., Williams, S., Fairhead, J., Ravat, D., & Smith, R. (2007). Tilt-Depth Method: A Simple Depth Estimation Method Using First-Order Magnetic Derivatives. *The Leading Edge, 26,* 1502-1505. https://doi.org/10.1190/1.2821934

Taskin, H., Karavus, M., Ay, P., Topuzoglu, A., Hidiroglu, S., & Karahan, G. (2009). Radio-Nuclide Concentrations in Soil and Lifetime Cancer Risk Due to Gamma Radioactivity in Kirklareli, Turkey. *Journal of Environmental Radioactivity, 100,* 49-53. https://doi.org/10.1016/j.jenvrad.2008.10.012

Telford, W. M., Geldart, L. P., & Sheriff, R. E. (1990). *Applied Geophysics* (2nd ed.).

Cambridge University Press. https://doi.org/10.1017/CBO9781139167932

Tzortzis, M., & Tsertos, H. (2004). Determination of Thorium, Uranium and Potassium Elemental Cocentrations in Surface Soils in Cyprus. *Journal of Environmental Radioactivity, 77,* 325-338. https://doi.org/10.1016/j.jenvrad.2004.03.014

UNSCEAR (2000). *Sources and Effects of Ionizing Radiation*. United Nation Scientific Committee on the Effects of Atomic Radiation Sources to the General Assembly with Annexes, Effects and Risks of Ionizing Radiation, New York: United Nations Publication.

UNSCEAR (2008). *Sources and Effects of Ionizing Radiation*. United Nation Scientific Committee on the Effects of Atomic Radiation Sources to the General Assembly with Annexes, Report to the General Assembly, with Scientific Annexes, New York: United Nations Publication.

WHO, World Health Organisation (2008). *Guidelines for Drinking-Water Quality, 3rd Edition in Cooperating the 1st Agenda Vol. 1 Recommendations; Radiological Aspect*. WHO.